Microsyst Technol (2012) 18:159–166
DOI 10.1007/s00542-011-1366-z

TECHNICAL PAPER

Micro fabrication of cyclic olefin copolymer (COC) based microfluidic devices

Rajeeb K. Jena · C. Y. Yue · Y. C. Lam

Received: 16 March 2011 / Accepted: 4 October 2011 / Published online: 18 October 2011
© Springer-Verlag 2011

Abstract Microfabrication of polymer using hot embossing technique are becoming increasingly important and considered as low-cost alternative to the silicon or glass-based micro-electro-mechanical systems technologies. This report is based on a parametric study on the hot embossing of cyclic olefin copolymer (COC) (Topas-6015 grade). The key process parameters in hot embossing such as the embossing temperature, load, the holding time and the demolding temperature significantly impact the quality of the embossed product. The work was performed to understand the influence of the various process parameters on the embossed micro-size patterns with the aim to develop the capability for microfluidic devices manufacturing. Microembossed polymer replicates were measured using a PLμ confocal microscope and inspected using a scanning electron microscope. It was established that the optimal embossing temperature for COC is 10°C above its T_g, while an optimal embossing load of 2.94 kN and holding time of 180 s are required. We have also demonstrated the effective sealing of the microchannel without destroying the channel integrity by thermal bonding technique.

1 Introduction

Microfluidic devices are widely used for various kinds of bio/chemical analyses. Microfluidic chip networks benefit from the increase in surface area to volume ratio accompanying miniaturization that translates into reduced chemical requirements, improved control, faster processing and tremendous potential for parallel processing and process integration. For example, a microfluidic system for DNA analysis might be formed by an array of channels 10–50 μm in depth and width, which utilizes microliter volumes of samples for the separation and detection of DNA molecules in nanomolar or picomolar concentrations. In the beginning, silicon was widely used for making microfluidic device due to the implementation of the micro-electro-mechanical systems (MEMS) fabrication processes (Lichtenberg et al. 2002). Structural integrity and dimensional control were good by using this material and these processes. However, the disadvantage of silicon is that its processing involves the use of wet and dry etching, photo-lithography, electron beam lithography, and a variety of other techniques, all of which require the use of clean room facilities and equipment. Glass based microfluidic devices are also popular due to their excellent optical properties, surface stability and their strong capillary and electroosmotic effects with water. However, the high cost involved in processing glass limits their usage as disposable devices. Therefore, there is much interest in utilizing alternative materials that are cheaper, such as polymers, for making microfluidic devices. Polymers are useful due to their wide range of material properties and surface chemistries which allows the substrate to be optimized according to the application. Moreover, polymers are cheap (necessary for a cheap disposable device) and can rapidly be manufactured through implementation of replication technologies for mass production (Studer et al. 2002; Vannahme et al. 2010; McCormick et al. 1997; Duffy et al. 1998; Gale 1997; Becker and Heim 2000; Shinohara et al. 2007; Mair et al. 2006; Seunarine et al. 2006;

R. K. Jena · C. Y. Yue (✉) · Y. C. Lam
Singapore-MIT Alliance, Manufacturing Systems and Technology Programme, Singapore, Singapore
e-mail: mcyyue@ntu.edu.sg

R. K. Jena · C. Y. Yue · Y. C. Lam
School of Mechanical and Aerospace Engineering, Nanyang Technological University, 50 Nanyang Avenue, Singapore 639798, Singapore

Wabuyele et al. 2001; Li et al. 2005; Fujii 2002). In this study, we have used cyclic olefin copolymer (COC) as the material of choice for fabrication of microfluidic device.

COC is a comparatively new thermoplastic material, and has been gaining esteem in LOC (Lab-on-chip) fabrication due to its better chemical properties (Nielsen et al. 2004). COC is a copolymer consisting of ethylene and norbornene that is synthesized using a metallocene catalyst. Through its characteristic molecular structure and superior catalyst technology, COC offers a wide range of grade variations, in terms of flow properties and heat resistance, such as Topas-8007 ($T_g = 78°C$), Topas-5013 ($T_g = 130°C$), Topas-6015 ($T_g = 160°C$) and Topas-6017 ($T_g = 130°C$). As a result, depending on the specific application, an appropriate substrate material can be selected for the microdevice. Thus, Topas-6015 and Topas-6017 would be more suitable for polymerease chain reaction (PCR) devices requiring higher heat resistant material. Moreover, due to the olefinic character, COC has good resistance to hydrolysis, acids and alkalis, and most organic polar solvents such as acetone, methanol, and isopropyl alcohol. It can be soluble in non-polar organic solvents such as toluene and naphtha. It is characterized as having high purity, good biocompatibility, excellent optical properties and high flowability. It has higher transparency in visible and near ultraviolet regions compared to poly(methyl methacrylate) (PMMA). The refractive index of COC is higher than that of PMMA, making COC ideally suited for applications that use optical detection methods. COC is easier to emboss, which is especially important when using soft PDMS tools because the density of COC is lower than that of PMMA. The water absorption of COC is $<0.01\%$ which is ten times less than that of PMMA. Thus, the relative humidity changes in the environment will not significantly affect devices replicated in COC. Overall, based on its material properties, COC is ideally suited for hot embossing fabrication of microfluidic chips and devices, especially if signal detection is performed spectroscopically (Becker and Gartner 2000; McDonald et al. 2000).

A diversity of methods exist for the fabrication of microfluidic devices such as wet etching, reactive ion etching, soft lithography, hot embossing, injection molding and laser ablation. In this article we have used the hot embossing technique for manufacturing Topas based microfluidic device because it provides numerous advantages, for instance relatively low cost for embossing tools, simple operation, uncomplicated process steps (e.g. less processing parameters and big process window) and high replication accuracy for small features. It also introduces less residual stress in the polymer because the polymer only stretches a very short distance from the substrate into the microcavity during embossing. The basic principle of hot embossing is that a polymer substrate is first heated above its glass transition temperature, T_g. A mold (or master) fabricated by MEMS technique is then pressed against the substrate, allowing the pattern to be fully transferred onto the substrate. As the stamp progresses into the substrate during embossing, the material displacement may be viscoelastic. Various idealized representations of the filling process have been presented (Scheer and Schultz 2001; Young 2005; Lei et al. 2005; Worgull et al. 2008; Juang et al. 2002a, b). The final and often most challenging phase of the embossing cycle is the separation of mold from the substrate which can cause warpage of the substrate and breakage of the silicon die. The key control parameters in hot embossing are the embossing temperature, load and time.

The objective of this work is to study the behavior of the COC (Topas-6015 grade) material during the hot embossing process, with the aim of providing an optimized manufacturing process for microfluidic devices. The focus of the experiments is on the effect of three important parameters, namely: embossing temperature, embossing load and embossing time on the formation of microchannels and then applying the optimized condition for fabrication of capillary electrophoresis (CE) chip followed by effective sealing.

2 Experimental

2.1 Sample preparation

In this study, Topas-6015 and Topas-5013 grade provided by TICONA was used. Both Topas 6015 and 5013 grades are glassy polymers at room temperature, with glass transition temperatures (T_g) of approximately 160 and 130°C respectively. Each substrate with a thickness of 1 mm was fabricated from Topas pellets using a Battenfeld injection molding machine and cut to 25 mm × 25 mm in size. A 1 mm thick Topas-6015 sheet was used as the substrate material to fabricate microchannel during hot embossing where as Topas-5013 sheet (1 mm) was used as the cover plate during thermal bonding to seal the microchannel.

2.2 Fabrication of Si mold

The dies were fabricated as follows. Initially, schematic diagrams of the channels were drawn using standard L-EDIT software. The image was printed onto a transparency with resolution greater than 25 μm and then placed on top of a silicon wafer with crystal orientation ⟨100⟩. The photomask contain an array of microchannels having 50 μm width and 100 μm spacing between the channels. A 10 μm thick AZ 9260 positive photoresist was deposited

using a spin coater having spin speed 1,500 rpm and spinning time 30 s on the surface of the wafer and then soft baked at 100°C for 4 min on a hot plate. Upon exposure to the UV light source (wavelength = 365 nm and intensity = 9.3 mW/cm^2) for 40 s, the photoresist was developed for 100 s, revealing the transferred image. The Deep Reactive Ion Etching (DRIE) process was then used to create a depth of approximately 22 μm in the silicon wafer. The height and width (top and bottom) of the positive image were controlled by the etching time. In our DRIE process we used SF_6—130 sccm, O_2—13 sccm, radio frequency (RF) power—800 W, etching time 12 s and passivate for 8 s by passing 100 sccm C_4F_8 gas. Furthermore, as a consequence of the DRIE process, the sidewalls of the micro-channels in the dies were found to be tapered slightly by 2° which facilitated removal of the polymer substrate from the die after hot-embossing. The tapering angle depends on the etching time, the gas flow rate, the RF power and the depth of the microchannel. Finally, the dies were treated with C_4F_8 gas for 2 min to create a thin layer of Teflon-like material on the sidewall surfaces (post-passivation) to reduce the friction between die and Topas substrate during de-molding. After dicing, the size of the mold was 20 mm × 20 mm and its thickness was 5 mm. The cross-sectional profile of the Si mold measured by confocal microscope is shown in Fig. 1.

2.3 Experimental setup

The hot embossing machine used was a bench top hydraulic press with a load capacity of 15 tons. It was fitted with two 100 mm diameter heated platens (top and bottom) and these were connected to a temperature controller. A thermocouple was embedded into the top and bottom platen. Cooling was achieved through natural air cooling and through water cooled plates attached to the platens. A chiller was connected to the hot embossing equipment to circulate water through the two cooling plates attached to the top and bottom platens.

2.4 Characterization of microchannels using interferometry

The 3D topography and channel profile (depth, top and bottom width) of the embossed channels were measured using a PLμ Confocal microscope. For each dimension, four measurements were taken and the average value was determined and plotted. The surface morphology was inspected using a scanning electron microscope (SEM). Throughout our studies, three key dimensions of the embossed microchannel, namely: the channel depth, top width and bottom width were determined.

3 Results and discussions

3.1 Effect of temperature on channel dimensions

To investigate the effect of embossing temperature, the temperature was varied from 160 to 175°C while keeping the embossing load (2.94 kN) and time (180 s) fixed. Figure 2 shows the results of percentage change in channel dimensions with varying temperature. It is clear from Fig. 2 that temperature has no significant effect on channel depth over the range of temperatures considered. In contrast, temperature had a significant effect on both the channel top and bottom widths. The variations in channel top and bottom widths were much higher at 160 and 165°C

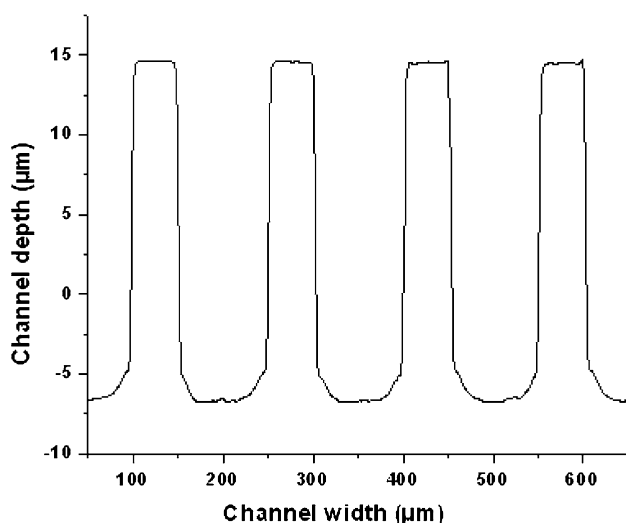

Fig. 1 Typical profile of cross-section of channel of Si Mold having 50 μm width and 100 μm spacing between the channels

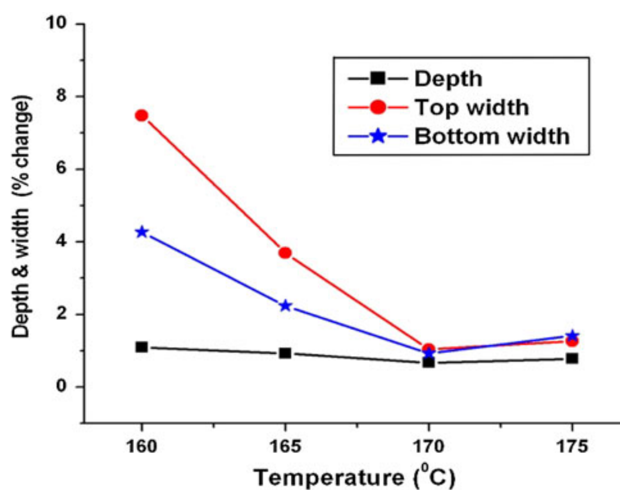

Fig. 2 Effect of embossing temperature on channel depth and width

than at 170 and 175°C. This is because the viscosity of Topas-6015 grade was higher at the lower temperatures and therefore cannot flow as easily to fill up the microcavities during embossing than at higher temperatures. Moreover, the lower polymer viscosity at higher temperatures enables the microcavities to be filled easily thus resulting in less variation in the top and bottom widths. At 170°C, excellent replication of the mold was obtained such that the variation in channel dimension was only about −1.2%. The variation in channel top and bottom width at 175°C is higher compared to that at 170°C. This may be due to the larger recovery of compressive elastic strain after demolding at 175°C.

3.2 Effect of embossing load on channel dimensions

To investigate the effect of embossing load on the replication process, the embossing load was varied form 1.46 to 2.94 kN whilst the embossing temperature (170°C) and time (180 s) were kept constant. It can be seen from Fig. 3 that the replication accuracy on channel dimensions increases as the embossing load was increased. The depth of the microchannel increased as the load was increased. Full replication of the channel depth was obtained when the applied force was at least 2.5 kN. For the channel top and bottom widths, the degree of replication also increased with embossing load. Excellent replication with dimensional variations of less than −0.98% was obtained when the load was 2.94 kN. This is not surprising because at lower embossing loads, the polymer cannot completely fill the microcavities resulting in variations in the replicated widths. Larger embossing loads are required to ensure complete filling of the microchannels resulting in better replication of the mold dimensions.

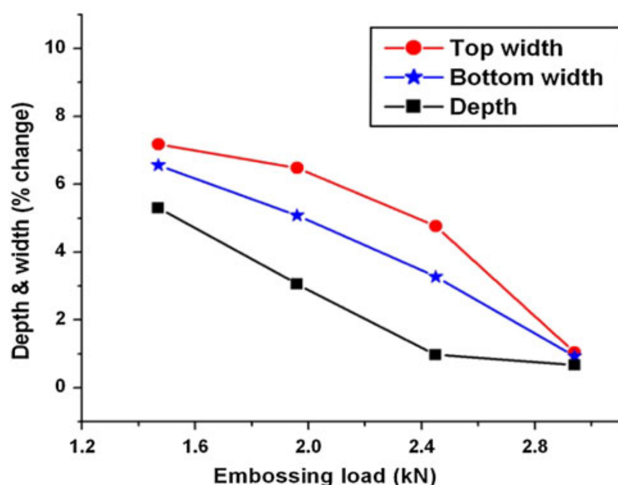

Fig. 3 Effect of embossing load on channel depth and width

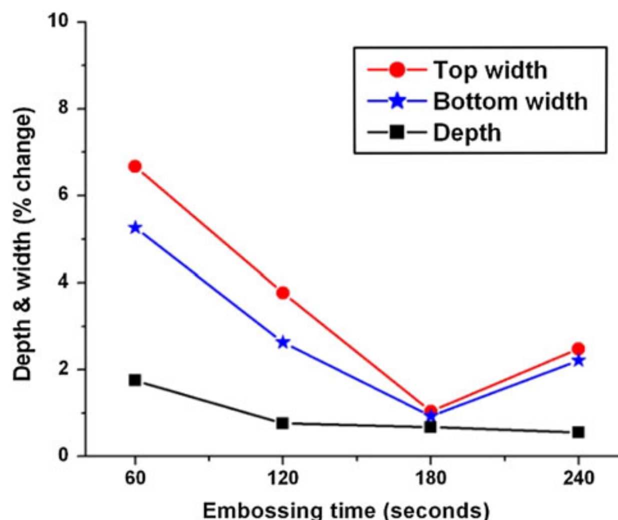

Fig. 4 Effect of embossing time (seconds) on channel depth and width

3.3 Effect of embossing time on channel dimensions

To investigate the effect of embossing time on the replication process, the embossing time was varied from 60 to 240 s whilst the embossing temperature (170°C) and load (2.94 kN) were kept constant. It is clear from Fig. 4 that the replication accuracy on all the three channel dimensions increases as the embossing time was increased and reached an optimum at 180 s. The replication accuracy decreased when the embossing time was more than 180 s. It can be seen from Fig. 4 that it was easier to replicate the depth compared to the microchannel widths. Full replication of the channel depth was obtained when the embossing time was at least 120 s. In comparison, the channel top and bottom widths were not fully replicated when the embossing time was 120 s but was achieved at 180 s. The longer embossing time required for replicating the channel top and bottom widths can probably be attributed to the necessity for a short duration of sustained pressure during the embossing process to enable complete packing and filling of the microcavities in the mold. This is an effect that is commonly observed in injection molding. The decreased degree of replication at an embossing time of 240 s implied that packing for prolonged durations can induce internal stresses in the melt state that led to higher shrinkage in the polymer substrate after release from the mold.

4 Fidelity of replication

In order to confirm that good replication fidelity could be obtained, a final set of embossing tests were carried out using the optimal embossing parameters i.e., 170°C embossing

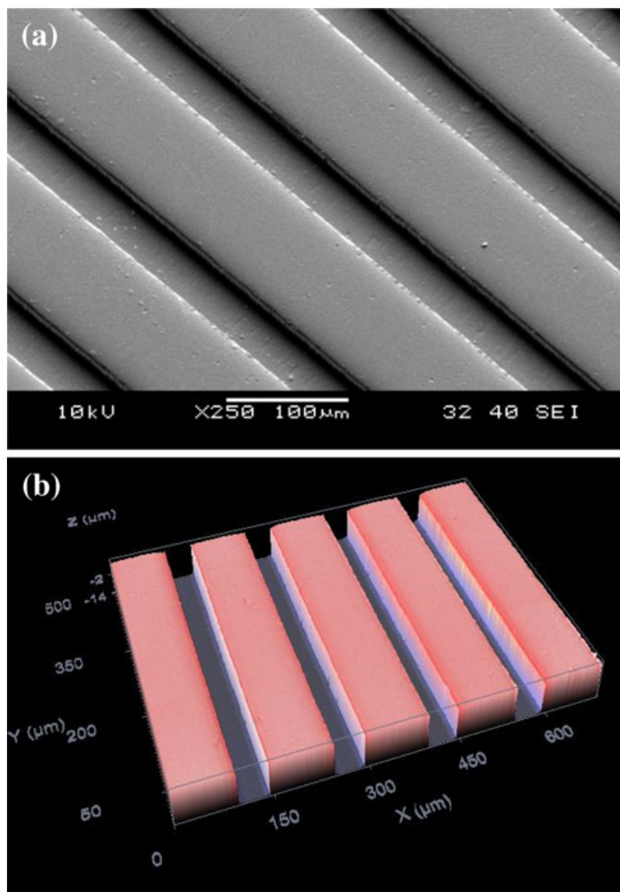

Fig. 5 Typical **a** SEM micrograph and **b** confocal image of embossed microchannels on Topas-6017 at optimized parameters. The embossing load was 0.5 kN and the embossing temperature was 170°C and embossing time for 180 s

temperature and 2.94 kN embossing load with an embossing time of 180 s which were determined in the above experiments. It can be seen from the SEM micrograph in Fig. 5a that micro-embossed features on the order of 20 μm high were transferred almost perfectly into the Topas substrate. The excellent replication was further confirmed using the optical profilometer image that is shown in Fig. 5b. Hence, it has been established that excellent replication of microchannels can be obtained using the micro-embossing technique.

We utilized the constitutive model of Srivastava et al. 2010 and showed that numerical predictions obtained using this model agreed well with the experimental profiles (Jena et al. 2010) obtained for the different hot-embossing conditions. Furthermore for thermal bonding near T_g, the deformation of the cover plate in the region of the microchannel could be predicted using a new modified creep model (Wang et al. 2010). Good agreement was obtained between the model prediction and the experimental data. These results are presented separately elsewhere (Jena et al. 2010; Wang et al. 2010).

5 Device fabrication and testing

After optimizing the microfabrication process for a simple array of microchannel, we turn our attention to fabricate a CE microchip (see Fig. 6a) as well as a micromixer with a serpentine channel with the optimized conditions. As a result, a 1 mm thick COC (Topas-6015) substrate was hot embossed at 170°C using an embossing load of 2.94 kN and an embossing time of 180 s. In CE (Fig. 6a), the longer channel called the separation channel and the shorter channel called the injection channels were 100 μm wide and 60 μm deep (aspect ratio 0.6), while the overall dimension of the chip was 22 mm × 22 mm. Measurements using the confocal microscope and SEM revealed that the dimensions of all the channels were consistent and had good replication fidelity with that of the mold dimensions. At this embossing condition, the dimensions of the embossed channel vary less than 2% compared to the mold dimension. This can be illustrated by the topography of the crisscross channel (see Fig. 6b, c, d) in the CE microchip.

The CE chip (Topas-6015, $T_g = 160$°C) was then sealed with another 1 mm thick cover plate made by injection molding of Topas-5013 ($T_g = 130$°C) by thermal bonding using the processing conditions given in Table 1. The point worth noting is that in thermal bonding, using a higher T_g material as the microchannel plate and a lower T_g material as the cover plate is an ideal choice because there will not be any deformation of the microchannel in the bottom plate in comparison to bonding two substrates having the same T_g. In general, during thermal bonding we need to heat the polymer above T_g so that the polymer chain can diffuse across the interface between the adjoining substrates to give a good bond. The likelihood of deforming both the cover plate and the microchannel in the base substrate plate is higher while bonding two substrate materials of the same T_g. In the case of using two substrate materials having slightly different T_g, bonding just above the T_g of the cover plate which has lower T_g will not result in any significant deformation of the microchannel in the base substrate plate. For this reason, we have selected two different materials for sealing the microchannel. The total time taken to fabricate one complete CE chip which includes both hot embossing as well as thermal bonding was 30 min.

Fluorescent dye solution was then passed through the CE device (see Fig. 7) in order to ensure that fluid can pass through the channel. In order to demonstrate the bond strength of the CE device, burst pressure measurements were carried out using a microLC pump (Teledyne Isco D-Series Pump Controller) fitted with a pressure transducer with an error accuracy of 0.5% over the range of 0–69 MPa. Before performing the burst test, a PEEK NanoPort assembly (Science Team Services, Singapore) was glued at four reservoirs of the CE chip onto the

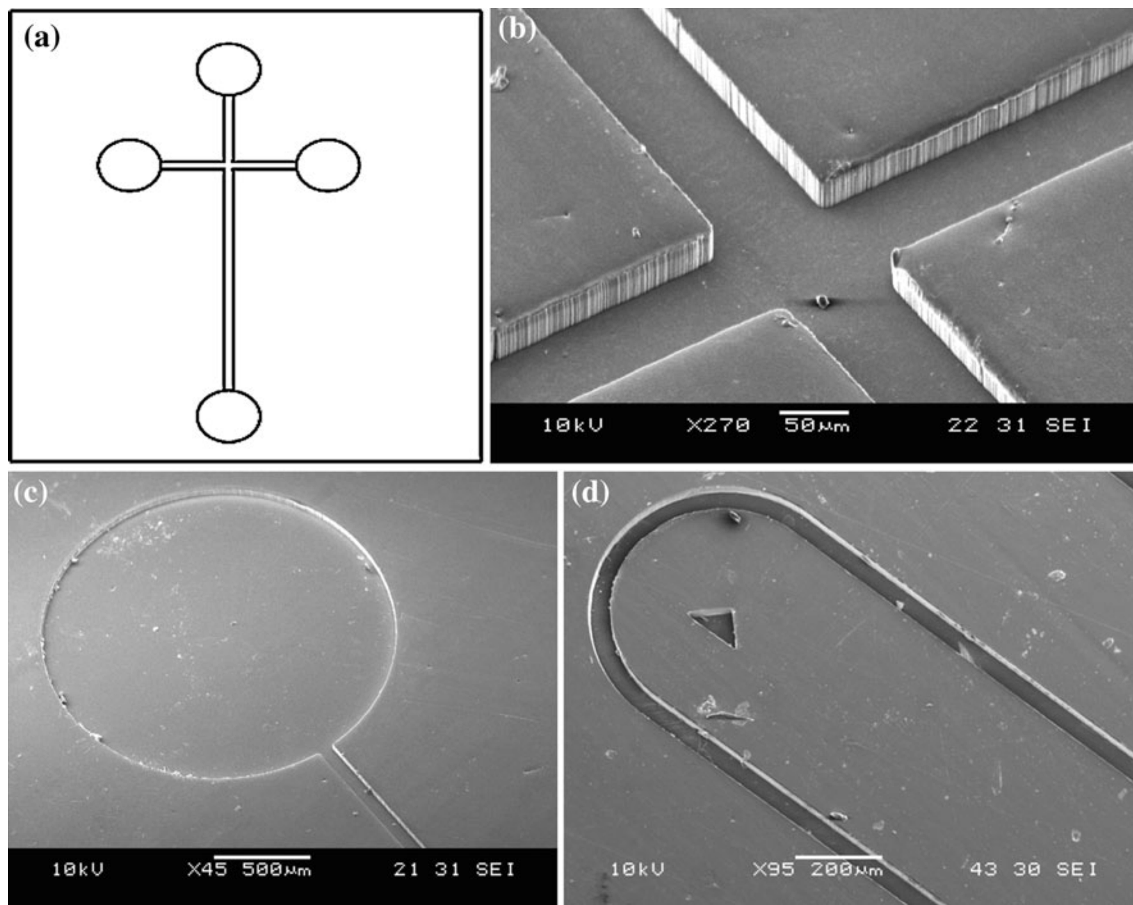

Fig. 6 **a** Schematic diagram of capillary electrophoresis chip **b** SEM micrograph of criss-cross micro channel; **c** reservoir micrograph of the capillary electrophoresis chip and **d** serpentine microchannel in micromixer in a micro-hot-embossed Topas-6017 part. The embossing load was 0.5 kN and the embossing temperature was 170°C and embossing time for 180 s

Table 1 Bonding parameters and burst pressure measurement results for each bonding conditions of the thermally sealed capillary electrophoresis chip

Trial	Temperature (°C)	Load (kN)	Time (min)	Burst Pressure (MPa)
1	120	0.5	2	1.6 ± 0.3
2	125	0.5	2	2.1 ± 0.4
3	125	0.5	4	2.8 ± 0.2
4	125	0.5	6	3.2 ± 0.6

thermally bonded plates using Araldite epoxy adhesive. After applying the epoxy adhesive, the substrates and the port were clamped for 24 h at room temperature. After that, it was then connected to the syringe pump via a natural fluoroethylene propylene (FEP) tube with a polyether ether ketone (PEEK) zero-dead-volume (ZDV). The ZDV union is fit for connecting 1/16″ OD tubing and is pressure rated to 41.4 MPa. Then water was passed through one reservoir to flow through the channel by blocking the other three reservoirs using the plug. The water flow rate was set at 0.05 mL/min and the burst pressure was recorded using the pressure transducer. The burst pressures at different bonding conditions are given in Table 1, indicating that a functional CE device can be obtained. Finally, the integrity of the device was checked by measuring the channel profile at different bonding conditions using the confocal microsope after manually separating the cover plate from the bottom plate. It was observed that bonding at 125°C, using 0.5 kN load for 6 min gave the highest burst pressure without any deformation in the microchannel.

We have also taken into consideration the other challenges such as resolution, aspect ratio and the throughput of the devices while fabricating microchips using hot embossing technique. It was observed that it is very difficult to replicate an array of microchannels (each having 25 µm width and 60 µm depth) when the spacing between adjacent microchannels was 25 µm at 170°C embossing temperature and 2.94 kN embossing load with an embossing time of

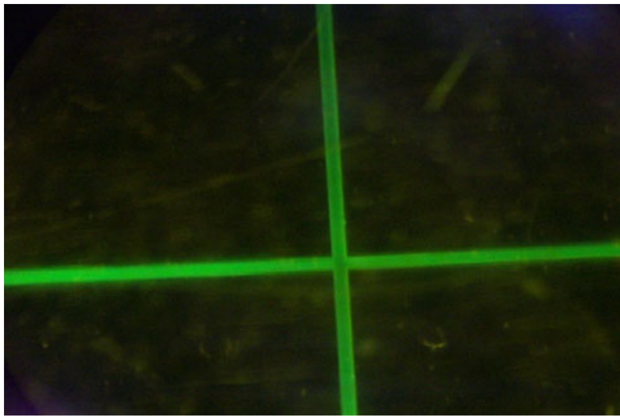

Fig. 7 Fluorescent dye solution passing through the capillary electrophoresis chip bonded by thermal bonding technique

180 s. This clearly indicates that replication fidelity also depends on the spacing between adjacent microchannels. We also studied the replication fidelity of microchannels with aspect ratios from 0.4 to 1.5. When the aspect ratio exceeded 1, the chances of mold breaking was very high, even after embossing only for one time because the mold broke during demolding due to adhesion of the substrate to the mold. The throughput of the device depends on the heating and cooling cycle of the hot embossing equipment and can be increased using a semi-automated process that has been developed by other members (Anthony et al. 2010) of our research program. By using semi-automated process the throughput of the device can be reduced to 5–10 min rather than 30 min.

Such devices could lead to the production of low-cost, single-use electrophoretic chips suitable for a variety of applications including DNA sizing, DNA sequencing, random primary library screening, rapid immunoassay testing, separation of proteins/peptides and identification of cells from a mixture. Adsorption of biomacromolecules on channel walls is a common problem for most microfluidic devices fabricated directly from commodity polymeric materials, which results in sample loss and deterioration in separation performance. Therefore, surface modification of the polymer surface is essential for generating new functionalities in the polymers in order to improve its hydrophilicity, bio-compatibility and antistatic adhesion. Several methodologies have been employed for improving the surface characteristics of polymers, out of which photografting and RF plasma are the potential technologies with wide industrial applications.

6 Conclusions

We have demonstrated the fabrication of microchannel on COC (Topas-6015 grade) substrate through hot embossing technique which allows low cost, flexible fabrication of polymeric Microsystems. Excellent replication could be obtained when the COC embossing parameters, including temperature, force and time were optimized. For Topas-6015, excellent replication was obtained when the embossing force, the embossing temperature and embossing time were 2.94 kN, 170°C and 180 s respectively. We have also demonstrated the effective sealing of microchannel without destroying the channel integrity by thermal bonding with introducing two different grades of the same materials (COC). Effective sealing was obtained at 125°C bonding temperature using 0.5 kN load for 6 min.

References

Anthony BW, Hardt DE, Hale M, Zarrouati N (2010) A research factory for polymer microdevices: muFac. In: Holger Becker, Wanjun Wang (eds) Microfluidics, BioMEMS, and medical microsystems VIII. California, SPIE, 2010. 75930A-12. ©2010 SPIE—The International Society for Optical Engineering

Becker H, Gartner C (2000) Polymer microfabrication methods for microfluidic analytical applications. Electrophoresis 21:12–26

Becker H, Heim U (2000) Hot embossing as a method for the fabrication of polymer high aspect ratio structures. Sens Actuators A 83:130–135

Duffy DC, McDonald JC, Schueller OJA, Whitesides GM (1998) Rapid prototyping of microfluidic systems in polydimethylsiloxane. Anal Chem 70:4974–4984

Fujii T (2002) PDMS-based microfluidic devices for biomedical applications. Microelectron Eng 61–62:907–914

Gale MT (1997) Replication techniques for diffractive optical elements. Microelectron Eng 34:321–339

Jena RK, Chester SA, Srivastava V, Yue CY, Anand L, Lam YC (2010) Large strain thermo-mechanical behaviour of a cyclic olefin copolymer (TOPAS) with application to hot embossing and thermal bonding for the fabrication of microfluidic devices. Sens Actuators B: Chem 155:93–105

Juang YJ, Lee LJ, Koelling KW (2002a) Hot embossing in microfabrication. Part I: Experimental. Polymer Eng Sci 42:539–550

Juang YJ, Lee LJ, Koelling KW (2002b) Hot embossing in microfabrication. Part II: Rheological characterization and process analysis. Polymer Eng Sci 42:551–566

Lei K, Li W, Yam Y (2005) Effects of contact-stress on hot-embossed PMMA microchannel wall profile. Microsyst Technol 11:353–357

Li C, Yang Y, Craighead HG, Lee KH (2005) Isoelectric focusing in cyclic olefin copolymer microfluidic channels coated by polyacrylamide using a UV photografting method. Electrophoresis 26:1800–1806

Lichtenberg J, de Rooij NF, Vepoorte E (2002) A microchip electrophoresis system with integrated in-plane electrodes for contactless conductivity detection. Electrophoresis 23:3769–3780

Mair DA, Geiger E, Pisano AP, Frechetacd JMJ, Svec F (2006) Injection molded microfluidic chips featuring integrated interconnects. Lab Chip 6:1346–1354

McCormick RM, Nelson RJ, Alonso MG, Benvegnu DJ, Hooper HH (1997) Microchannel electrophoretic separations of DNA in injection molded plastic substrate. Anal Chem 69:2626–2630

McDonald JC, Duffy DC, Anderson JR, Chiu DT, Wu H, Schueller OJA, Whitesides GM (2000) Fabrication of microfluidic systems poly(dimethylsiloxane). Electrophoresis 21:27–40

Nielsen T, Nilsson D, Bundgaard F, Shi P, Szabo P, Geschke O, Kristensen A (2004) Nanoimprint lithography in the cyclic olefin copolymer, Topas, a highly ultraviolet-transparent and chemically resistant thermoplast. J Vac Sci Technol B: Microelectron Nanometer Struct 22:1770–1775

Scheer HC, Schultz H (2001) A contribution to the flow behaviour of thin polymer films during hot embossing lithography. Microelectronic Eng 56:311–332

Seunarine K, Gadegaard N, Riehle MO, Wilkinson CDW (2006) Optical heating for short hot embossing cycle times. Microelectron Eng 83:859–863

Shinohara H, Mizuno J, Shoji S (2007) Fabrication of a microchannel device by hot embossing and direct bonding of poly (methyl methacrylate). Jpn J Appl Phys 46:3661–3664

Srivastava V, Chester SA, Ames N, Anand L (2010) A thermo mechanically-coupled large- deformation theory for amorphous polymers in a temperature range which spans their glass transition. Int J plasticity 26:1138–1182

Studer V, Pepin A, Chen Y (2002) Nanoembossing of thermoplastic polymers for microfluidic applications. Appl Phys Lett 80:3614–3616

Vannahme C, Christiansen MB, Mappes T, Kristensen A (2010) Optofluidic dye laser in a foil. Opt exp 18:9280–9285

Wabuyele MB, Ford SM, Stryjewski W, Barrow J, Soper SA (2001) Single molecule detection of double-stranded DNA in poly (methylmethacrylate) and polycarbonate microfluidic devices. Electrophoresis 21:3939–3948

Wang ZY, Yue CY, Lam YC, Roy S, Jena RK (2010) A modified quasi-creep model for assessment of deformation of Topas COC substrates in the thermal bonding of microfluidic devices. J App Polym Sci 122:867–873

Worgull M, Kabanemi KK, Marcotte JP, Hétu JF, Heckele M (2008) Modeling of large area hot embossing. Microsyst Technol 14:1061–1066

Young W (2005) Analysis of the nanoimprint lithography with a viscous model. Microelectron Eng 77:405–411